



Article

Novel Water-Soluble Poly(terephthalic-co-glycerol-g-fumaric acid) Copolymer Nanoparticles Harnessed as Pore Formers for Polyethersulfone Membrane Modification: Permeability–Selectivity Tradeoff Manipulation

Khalid T. Rashid ¹, Haiyam M. Alayan ¹, Alyaa E. Mahdi ¹, Mohammad N. AL-Baiati ², Hasan Sh. Majdi ³, Issam K. Salih ³, Jamal M. Ali ¹ and Qusay F. Alsalhy ^{1,*}

- ¹ Membrane Technology Research Unit, Chemical Engineering Department, University of Technology, Alsinaa Street 52, Baghdad 10066, Iraq; 80007@uotechnology.edu.iq (K.T.R.); hayomchm@yahoo.com (H.M.A.); alyaa.e.mahdi@uotechnology.edu.iq (A.E.M.); jamal.m.ali@uotechnology.edu.iq (J.M.A.)
- ² Department of Chemistry, College of Education for Pure Sciences, University of Kerbala, Kerbala 56001, Iraq; mohammad.nadhum@uokerbala.edu.iq
- ³ Department of Chemical Engineering and Petroleum Industries, AlMustaqbal University College, Babylon 51001, Iraq; dr.hasanshker@mustaqbal-college.edu.iq (H.S.M.); dr_issamKamil@mustaqbal-college.edu.iq (I.K.S.)
- * Correspondence: qusay.f.abdulhameed@uotechnology.edu.iq



Citation: Rashid, K.T.; Alayan, H.M.; Mahdi, A.E.; AL-Baiati, M.N.; Majdi, H.S.; Salih, I.K.; Ali, J.M.; Alsalhy, Q.F. Novel Water-Soluble Poly(terephthalic-co-glycerol-g-fumaric acid) Copolymer Nanoparticles Harnessed as Pore Formers for Polyethersulfone Membrane Modification: Permeability–Selectivity Tradeoff Manipulation. *Water* **2022**, *14*, 1507. <https://doi.org/10.3390/w14091507>

Academic Editors: Zhe Yang and Peng-Fei Sun

Received: 18 April 2022

Accepted: 6 May 2022

Published: 8 May 2022

Publisher's Note: MDPI stays neutral with regard to jurisdictional claims in published maps and institutional affiliations.



Copyright: © 2022 by the authors. Licensee MDPI, Basel, Switzerland. This article is an open access article distributed under the terms and conditions of the Creative Commons Attribution (CC BY) license (<https://creativecommons.org/licenses/by/4.0/>).

Abstract: This work presents poly(terephthalic-co-glycerol-g-fumaric acid) (TGF) as a novel water-soluble polymeric nano-additive for the modification of a polyethersulfone ultrafiltration membrane. The TGF was harnessed as a pore former, aiming to improve the membrane surface porosity and hydrophilicity. Modified membranes were characterized to observe the influence of varying the TGF content on their hydrophilicity, porosity, morphological structure, and composition, as well as their entire performance. The results disclosed that porosity and hydrophilicity of the modified membrane prepared using 4 wt.% TGF content recorded an enhancement by 24% and 38%, respectively. Herein, the lower contact angle was mainly a reflection of the improved porosity, but not of the hydrophilic nature of water-soluble TGF. Furthermore, upon increasing the TGF content in the polymeric matrix, a more porous structure with longer finger-like micropores was formed. Moreover, a sponge-like layer clearly appeared near the bottom surface. Nevertheless, at optimum TGF content (4%), a clear enhancement in the water flux and BSA retention was witnessed by values of 298 LMH and 97%, respectively. These results demonstrate that the obtained permeation and separation behavior of the PES/TGF membrane could stand as a promising choice for water and wastewater treatment applications.

Keywords: nano graft copolymer (TGF); polyethersulfone; wastewater; bovine serum albumin; ultrafiltration

1. Introduction

The lack of freshwater resources, along with the growing demand due to human and industrial activities, necessitates an urgent reaction. In most circumstances, these resources are contaminated and cannot be accessed directly, requiring further treatment. With the wide spectrum of available treatment techniques, membrane processes offer an exceptional solution to eliminate a variety of contaminants at a minimal feasible cost [1]. One of the prominent membrane processes that combine high permeability, high retention to disparate species, and low energy consumption is ultrafiltration (UF). With unique separation possibilities, UF has easily demonstrated its efficiency in many industrial applications for pathogen separation, sterilization, pharmaceutical production, food and juice concentration, and wastewater treatment [2]. Like other membrane processes, UF suffers from a

rapid flux depletion under industrial operations, due to versatile fouling mechanisms. In addition to the feed type, operational conditions, and feed chemistry, UF membrane surface characteristics are critical to diminish the fouling consequences.

Membrane surface modifications have been suggested as exceptional routes to partially resolve performance decline. All these methodologies are intended to enhance the performance of the target membrane by enhancing its hydrophilicity and surface morphology characteristics. Blending with hydrophilic additives is a common way to achieve this goal [3,4]. Limitless organic and inorganic additives and surface modification techniques have been reported in the literature since the introduction of the first fabricated membrane [5–8]. Among these additives, hydrophilic nanoscale materials have witnessed a surging interest. These materials can exhibit extraordinary features at their nanoscale level. However, the economic and environmental costs of using these nanomaterials for membrane modification are still under argument. The leaching of these nanomaterials out of the membrane structure is the biggest concern. This could not only waste these materials and cause environmental issues but also damage the membrane structure. Ultimately, this would deteriorate the overall membrane performance.

On other hand, the incorporation of water-soluble materials as pore-forming agents in the casting polymeric solution is another common approach to enhance the surface characteristics of the membrane. Additives to polymeric solutions, such as poly(vinyl pyrrolidone) (PVP), methylcellulose, glycerin, LiCl, ZnCl₂, and polyethylene glycol (PEG), have been investigated as pore-forming agents for enhancing membrane properties [9]. It is well known that adding pore-forming additives to the casting solution produces membranes with higher pore density, narrower pore size distribution, and higher porosity, along with boosting other structural properties that differ from those of the pristine membrane [10]. Polyvinylpyrrolidone (PVP) and poly (ethylene glycol) (PEG) are commonly employed as polymer blends due to their distinct effects on membrane surface properties and, thus, on the permeation and separation characteristics [11]. Zhao et al. (2011) [12] used the poly(ethylene glycol) methyl ether-*b*-poly (styrene) copolymers (mPEG-*b*-PS) to improve the hydrophilicity of PES hollow fiber. In another study conducted by Shi et al. (2013) [13], a novel hydrophilic poly(glycidyl methacrylate) (graft glycopolymer) was blended as an additive in the polysulfone (PSF) polymeric solution, aiming to improve the hydrophilic characteristic of the PES surface. Recently, dual pore-forming materials have been preferred to modify the structural morphology, physical features, and membrane separation performance of the polymer solution. For example, the impacts of PVP and hydroxypropyl-beta-cyclodextrin (HP-β-CD), as dual pore-forming additives in the PSF solution, on the characteristics and membranes performance were evaluated by Alayande et al. [14]. A significant enhancement was found in the membrane porous structure, hydrophilicity, and mechanical properties.

In this context, ecofriendly polymeric nanomaterials could provide an exceptional option to replace the conventional nanomaterials used for membrane modification. These types of novel nanomaterials are prepared by the graft copolymerization process [15]. Herein, our study reports for the first time the fabrication and application of a novel water-soluble nano-polymer (TGF) as a pore-forming agent with hydrophilic nature. A comprehensive characterization of the modified PES membranes was conducted to investigate the role of the TGF loading ratio on the permeation/retention characteristics of PES/UF membranes. Bovine serum albumin (BSA) was employed as an organic protein model for investigating the rejection behavior.

2. Experimental Method

2.1. Materials

PES polymer as a host membrane material with a density of 1370 kg/m³, BSA protein, terephthalic acid, glycerol, fumaric acid, xylene, and dimethyl sulfoxide (DMSO), as a solvent for the preparation of the membrane dope solution, were bought from Sigma Aldrich, Germany.

2.2. Preparation of Nano Poly(terephthalic-co-glycerol-g-fumaric acid) Solution

An amount of 332 g of terephthalic acid was dissolved in 50 cc of DMSO solvent in a 0.2 L double-necked round-bottom beaker. The beaker was provided with a quick-fit thermometer to maintain the temperature. By utilizing a hot plate magnetic stirrer, the mixture was warmed carefully up to 40 °C, until a clear liquor was formed. Subsequently, 92 g of glycerol was added to the solution. The new mixture was heated to about 120 °C and xylene (25 mL) was added meticulously to the reaction beaker by batches (drop by drop). The water produced from the esterification process was withdrawn, and the beaker was then heated. The main reason for adding *p*-xylene to the solution was to remove the water formed as a byproduct of the esterification reaction process during the preparation of the nano copolymer. Heating was applied for 80 min at 145 °C, and the reaction beaker was left to cool to 50 °C. Fumaric acid (58 g) was dissolved in 10 cc of DMSO solvent at 40 °C and then added to the mixture (readymade in the first stage). The reaction beaker was heated carefully up to 100 °C, and then xylene drops were added by batches (two drops each time) (with continuous heating for 45 min) at 115 °C, until no more water was produced. The beaker was left to cool down to the ambient temperature, and then distilled water was added. The formed suspension solution was allowed to precipitate, filtered, washed with deionized water, and then left to dry (Figure 1).

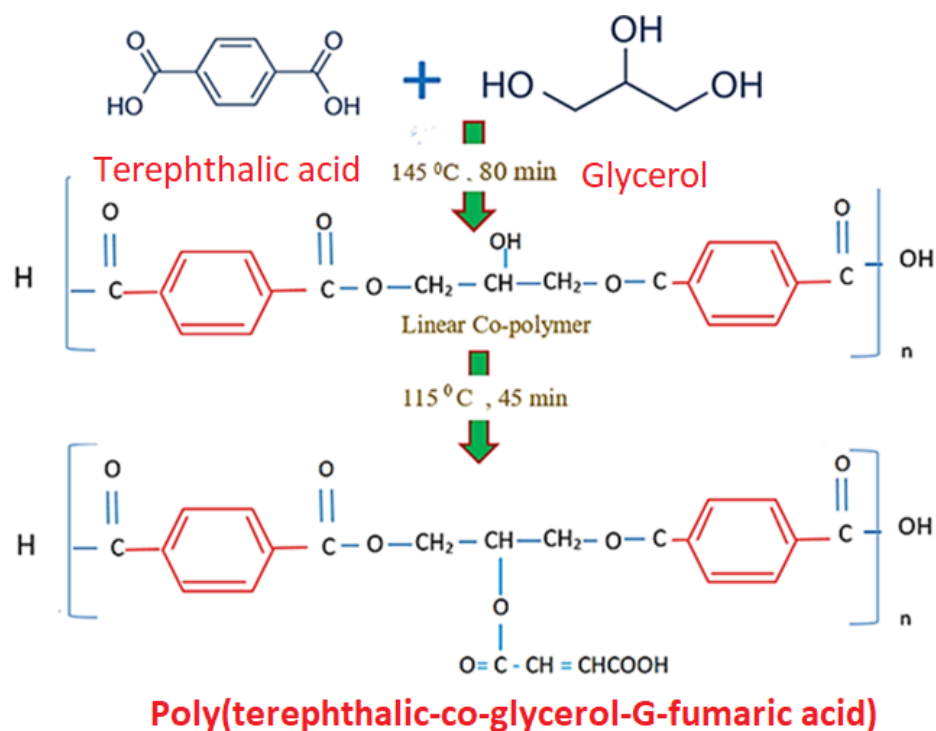


Figure 1. Reaction of terephthalic acid and glycerol for TGF graft polymer production.

2.3. TGF Characterization

Proton nuclear magnetic resonance (i.e., $^1\text{H-NMR}$) is the application of nuclear magnetic resonance spectroscopy with respect to hydrogen-1 nuclei inside the molecules of a material to define its molecular structure. $^1\text{H-NMR}$ spectral measurements were acquired on a Bruker DPX 300 device at 300.13 MHz for hydrogen nuclei in CDCl_3 , and all chemical shifts are presented in ppm.

2.4. Membrane Preparation

A porous, flat sheet, PES/TGF nano-polymer membrane was synthesized via adopting the phase inversion method. As mentioned in Table 1, 20 wt.% PES was blended with various concentrations of TGF nano-polymer and dissolved in DMSO. The casting polymer solutions were continuously mixed at 50 °C for 48 h to obtain a homogeneous dope solution.

Subsequently, the polymer casting solution was degassed, filtered, and cast onto a glass plate utilizing an automatic casting knife. Later, the membrane was submerged in a deionized water bath for coagulation. The formed membranes were rinsed thoroughly and stored in deionized water for further analysis.

Table 1. Composition of the prepared casting solutions of PES/TGF membranes.

Membrane Code	PES%	DMSO	TGF%
Go	20	80	0
G1	20	80	1
G2	20	80	2
G3	20	80	3
G4	20	80	4
G5	20	80	5
G6	20	80	6

3. Membrane Characterization

3.1. Fourier-Transform Infrared (FTIR) Spectroscopy

Fourier-transform infrared spectroscopy (FTIR, 8400 S, Br., Ettlingen, Germany) was utilized to detect the chemical compositions of the prepared membranes. The spectra were estimated with a wavenumber range of 400–5000 cm^{−1}.

3.2. Membrane Morphology

The morphology of the prepared membranes was scrutinized utilizing a scanning electron microscope (SEM) a TESCAN VEGA3 SB instrument (EO Elektronen-Optik-Service GmbH, Dortmund, Germany). The prepared sheets were first fractured by utilizing liquid nitrogen and subsequently sputtered with a thin coat of platinum before imaging the cross-sections.

3.3. Contact Angle Measurement

The membrane contact angle was evaluated employing the sessile drop method. The optical contact angle instrument (CAM110, Tainan, Taiwan) was employed as described elsewhere [16]. For each sample, at least five different locations of the contact angle test were taken, and the average value was estimated.

3.4. Membrane Porosity and Pore Size

Membrane specimens were cut off into 2 cm² size pieces and immersed in distilled water for 15 h. Wet membranes were removed from water; then, excess droplets were removed from the membrane surface utilizing a blotting paper and weighed. Using a vacuum oven for 12 h, the membranes were dried, and the dry samples were weighed. The membrane porosity was evaluated by Equation (1). For each membrane sample, five estimates of contact angle were taken, and the calculations were averaged.

$$\varepsilon(\%) = \left(\frac{W_w - W_d}{A \times l \times \rho} \right), \quad (1)$$

where W_w and W_d are the wet and dry weight values of the membrane, respectively, A is the membrane sample area (cm²), l is the membrane thickness (cm), and ρ is the water density (1 g/cm³).

The mean pore size (rm) was determined on the basis of membrane porosity and pure water flux using Equation (2).

$$rm = \sqrt{\frac{(2.9 - 1.75 \varepsilon) \times (8\eta l Q)}{\varepsilon \cdot A \cdot \Delta P}}, \quad (2)$$

where η is the water viscosity, Q is the collected volume of the pure water flux per unit time (m^3/s), ΔP is the operation pressure, ε is the membrane porosity, and l and A are the membrane thickness and effective area, respectively [17].

3.5. Membrane Performance

With an efficient area of 16 cm^2 , a cross-flow filtration system was employed to check the membrane performance at ambient temperature. Membrane permeation was analyzed with a pure water flux (PWF) and a 1000 ppm BSA solution. The permeate flux (J) was specified utilizing Equation (3) [18].

$$J = \frac{V}{A \times t}, \quad (3)$$

where V is the collected permeate volume (m^3) with the time (t), and A is the effective membrane area (m^2) in the filtration cell.

The BSA solution rejection was evaluated using Equation (4) [19].

$$R\% = \left(1 - \frac{c_p}{c_f}\right) \times 100. \quad (4)$$

4. Results and Discussion

4.1. Fourier-Transform Infrared Spectroscopy

FTIR spectra of the pure PES membrane and the modified membrane containing various concentrations of TGF nano-polymer are shown in Figure 2. As can be seen, the characteristic peaks of PES membranes, before and after adding the TGF nano-polymer, were characterized by absorption peaks at 1152 , 1147 , 1250 , and 1350 cm^{-1} , assigned to stretching bands of C–O, O=S=O, C–H, and O–H groups, respectively. Furthermore, the presence of a strong, broad band at 3424 cm^{-1} for a stretching alcoholic bond (–OH) was observed.

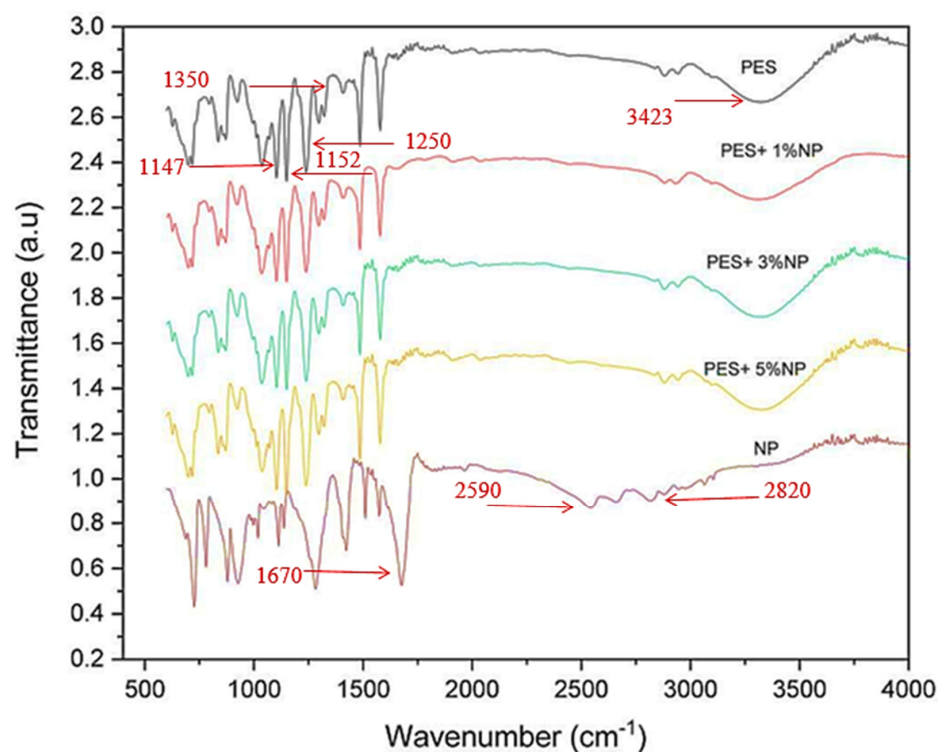


Figure 2. FTIR spectra of the bare PES and PES/TGF membranes.

It is worth mentioning that the comparison between the PES/TGF and the pure PES membrane spectra showed the presence of no unprecedented absorption bands. In addition, for the prepared PES/TGF membrane, a complete disappearance of the bands at 1670, 2590, and 2820 was clear, attributed to the addition of the nano-polymer. This is clear evidence that the TGF nano-polymer did not remain in the membrane matrix, or that it remained in very small quantities. This means that all TGF in the casting solution was removed during the phase inversion process in the water coagulation bath, and the amount of TGF was accumulated at the glass plate after fabrication of the PES/TGF membrane, as depicted in Figure 3. This explains the withdrawal of most of the TGF nano-polymer particles from the membrane structure toward the water bath coagulation (see Figure 3).

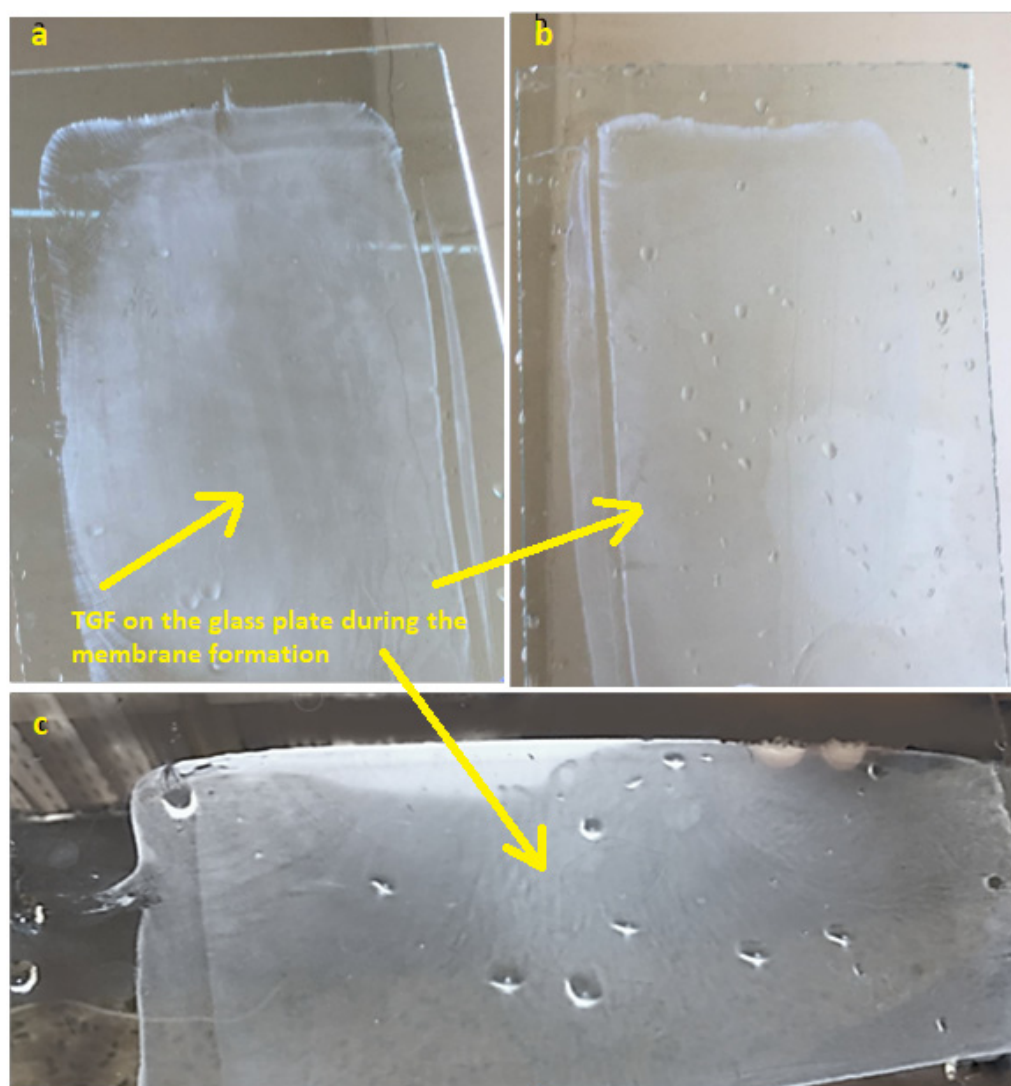


Figure 3. Glass plate of casting solution showing the amount of TGF nano-polymer remaining on the glass surface after formation of the membranes for (a) G1, (b) G3, and (c) G6.

4.2. Poly(terephthalic-co-glycerol-g-fumaric acid) Characteristics

Figure 4 clarifies the ^1H -NMR spectra of the TGF. The results demonstrate a singlet at 13.22 ppm, distinguishing the proton in a carboxylic acid group, multiplets at 7.5–8.5 ppm belonging to all aromatic ring protons, signals with 6.27–6.5 ppm for four protons of methylene in the polymer structure, and multiplets at 4.22–4.5 ppm for methyl protons. However, the triplet signal at 3.43–3.65 ppm belonged to the proton of the aliphatic alcohol. Accordingly, these spectra proved the formation of the targeted polymer.

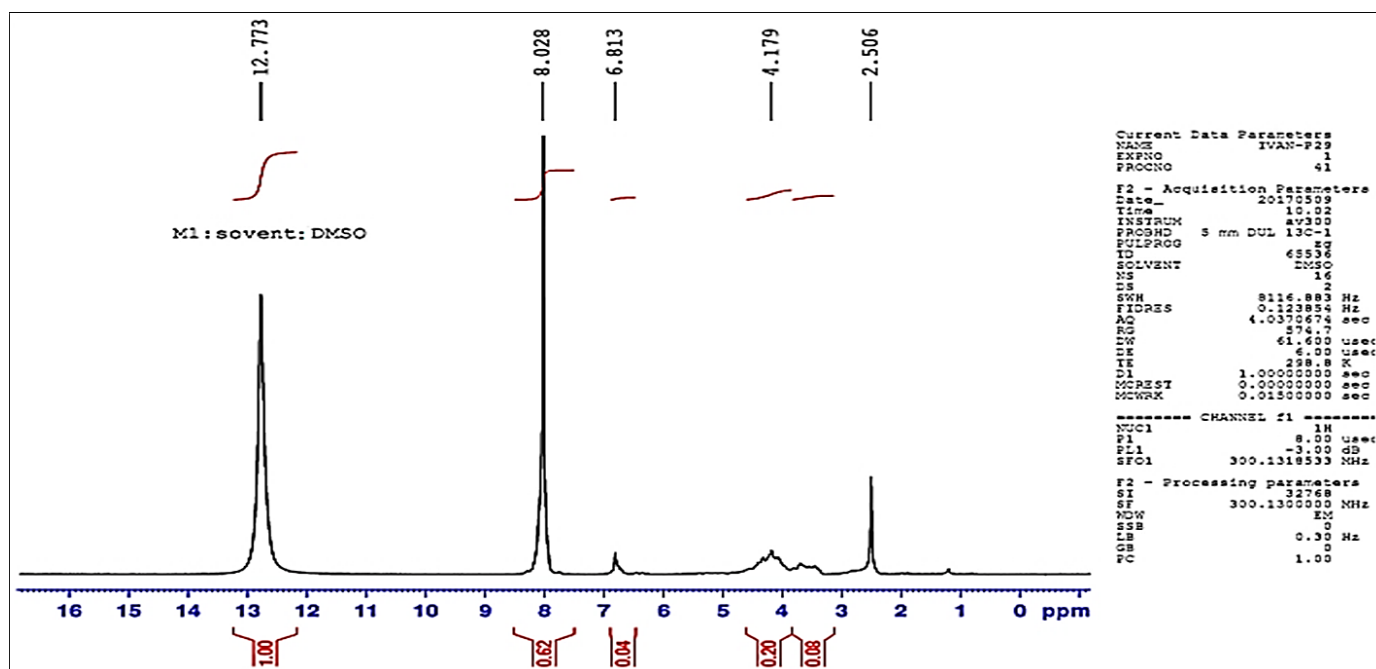


Figure 4. ^1H -NMR spectra of the prepared poly (terephthalic-co-glycerol-g-fumaric acid) nanoparticles.

Figure 5 illustrates the overall size ranges of the prepared TGF particles, as well as the various proportions of particle size distribution. The outcomes reveal that the polymer nanoparticle molecular mean size was 88.07 nm. The figure also elucidates the distribution of the various sizes ratios of nano-polymer nanoparticles.

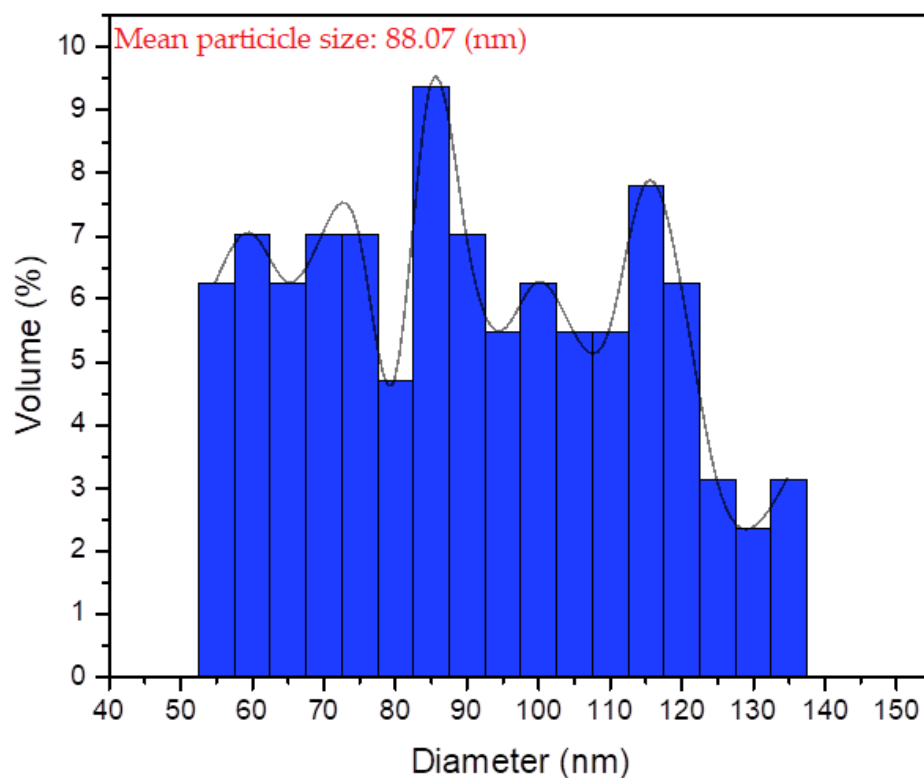


Figure 5. Various proportions of particle size distribution for TGF nanoparticles.

4.3. Effects of TGF Nano-Polymer on Membrane Morphology

SEM analysis is a substantial technical tool to inspect the morphology and structure of membranes, via which qualitative data regarding their surface and cross-sectional structures can be gained. Figure 6 illustrates the SEM photos of cross-sections from various flat sheet PES membranes prepared with diverse TGF contents. It can be observed that the prepared membranes had asymmetric structures composed of a porous sublayer (support layer) and a dense top surface layer (skin layer, air side). The skin layer (i.e., the effective layer) worked as a separation layer, while the membrane mechanical strength was provided by the support layer. The sublayer appeared with finger-like cavities below the top surface layer, along with wide voids close to the bottom surface layer. As can be noticed, the addition of the TGF nano-polymer in the polymer solution indeed played a role in altering membrane morphology. When the concentration of TGF nano-polymer increased, the number and the size of the finger-like pores increased. Larger and more prominent voids were also detected. It can be concluded from Figure 6 that the TGF worked as a pore former in the process of membrane structure formation. It can also be noticed that, when the TGF nano-polymer was added to the casting solution, the thickness of the dense layer receded slightly. The finger-like pores progressively lengthened to the bottom of the membrane at the expense of the dense layer. This variation is obvious in Figure 6G1, where it can be clearly seen that the tiny finger-like pores of the pure membrane were altered to larger finger-like cavities. Furthermore, larger pores were formed through the sublayer of the synthesized membrane cross-structure. Through the membrane cross-structure, these channels evolved from top to the bottom and joined each other via sponge-shaped partitions. It is noteworthy that, when the content of TGF nano-polymer in the doping solution was higher than 5%, an increase in the viscosity of the polymer solution and a transfer of the nano polymer particles (through the membrane) toward the bottom layer were observed through the casting operation. This in turn led to a comparatively denser and thicker active layer formed near the bottom surface of the PES membrane, as clearly shown in Figure 6G6. All of these events occurred because of the effectiveness of the TGF hydrophilic polymer, which enhanced the thermodynamic instability of the casted polymeric membrane. These outcomes are consistent with those found by Farjami et al. [20]. The porous bulk acts only as a mechanical support layer, whereas the skin layer is accountable for the permeation and solute retention [21–23].

The alteration in the size and the enhanced mean pore size (Figure 6) and pore density (Figure 7) as a result of the presence of TGF in the membrane matrix could be interpreted as two major observations: (a) the dissolution of TGF induced higher polymer concentration and, ultimately, higher viscosity of the dope solution; (b) the polymer-doped solution became less thermodynamically stable, which resulted in a delay in the demixing process when the membrane dope solution was immersed into the coagulation bath. The hydrophilicity of TGF particles in the membrane solution influenced the solvent/nonsolvent rate exchange through the phase inversion operation. It also impacted the precipitation kinetics and the formation of the produced membrane structure. Similar observations were demonstrated in previous studies [24,25].

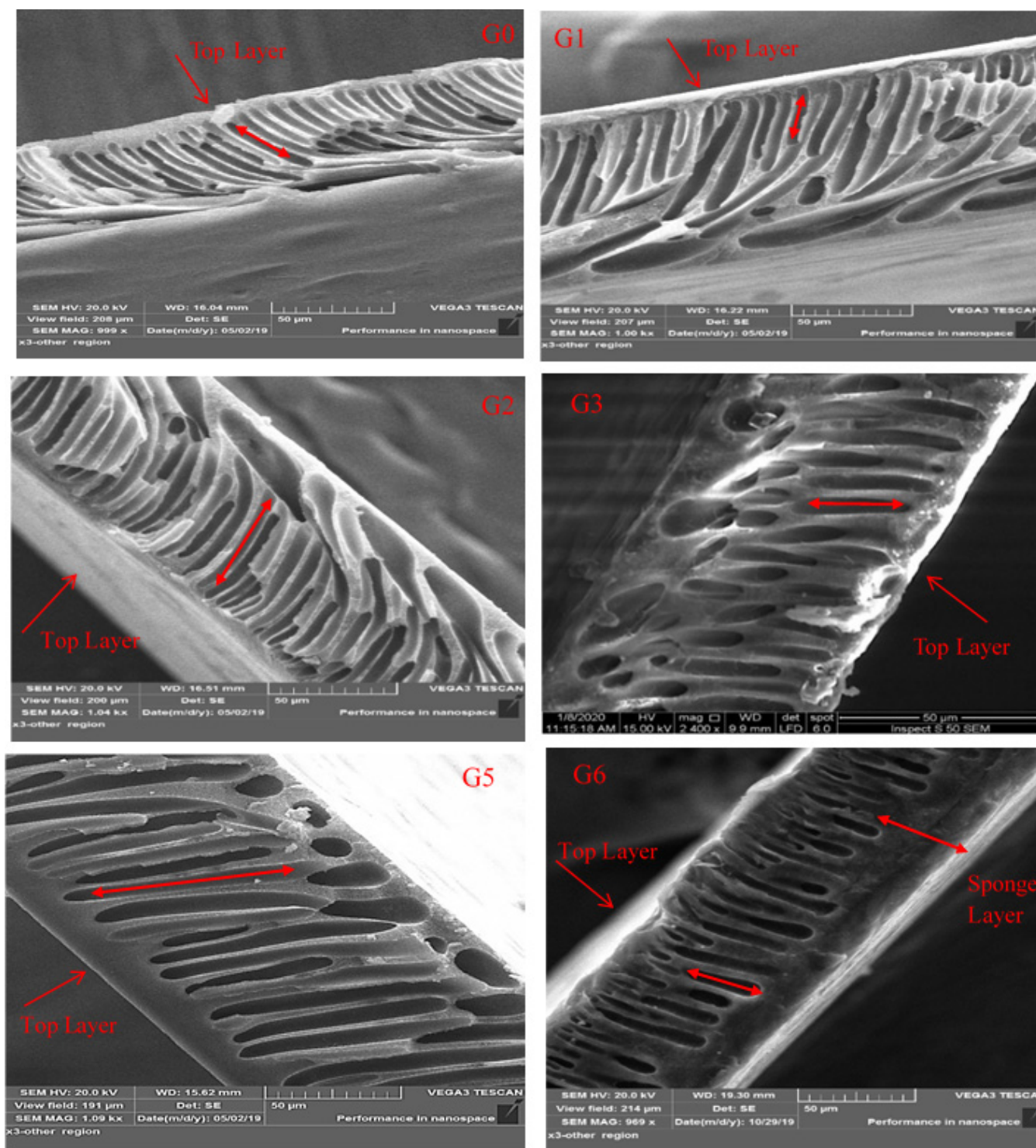


Figure 6. SEM images for the cross-section structures of the neat and PES/TGF membranes with various contents of TGF nano-polymer ((G0) 20/0, (G1) 20/1, (G2) 20/2, (G3) 20/3, (G5) 20/5, (G6) 20/6).

Figure 7 presents the top surface SEM photos of the PES membranes synthesized with various TGF blend contents. After blending the TGF nano copolymer into the dope solution, it can be clearly noted that pores were formed at the skin layer (Figure 7G1). The increase in the concentration of TGF nano-polymer in the polymeric solution resulted in an effective improvement in the density of the pore. It should be observed that small

quantities of TGF were sufficient to start pore formation in the membrane skin layer. Since the skin layer controls membrane selectivity, there is likely to be strict control over the performance of the membrane by adding TGF in the dope solution, as clarified in the subsequent paragraph. The increase in membrane porosity with the addition of TGF can be explained by the aggregation of TGF in the casting membrane/water interface, through the pervaporation phase and the pore-forming impact of TGF after immersing the casting membrane into the coagulation bath. However, when the TGF concentration was higher than 4.0 wt.%, membrane porosity stopped increasing and declined slightly. This may have been a result of increased viscosity of the dope solutions, which impeded the nano-polymer particle movement and limited the formation and development of membrane pores.

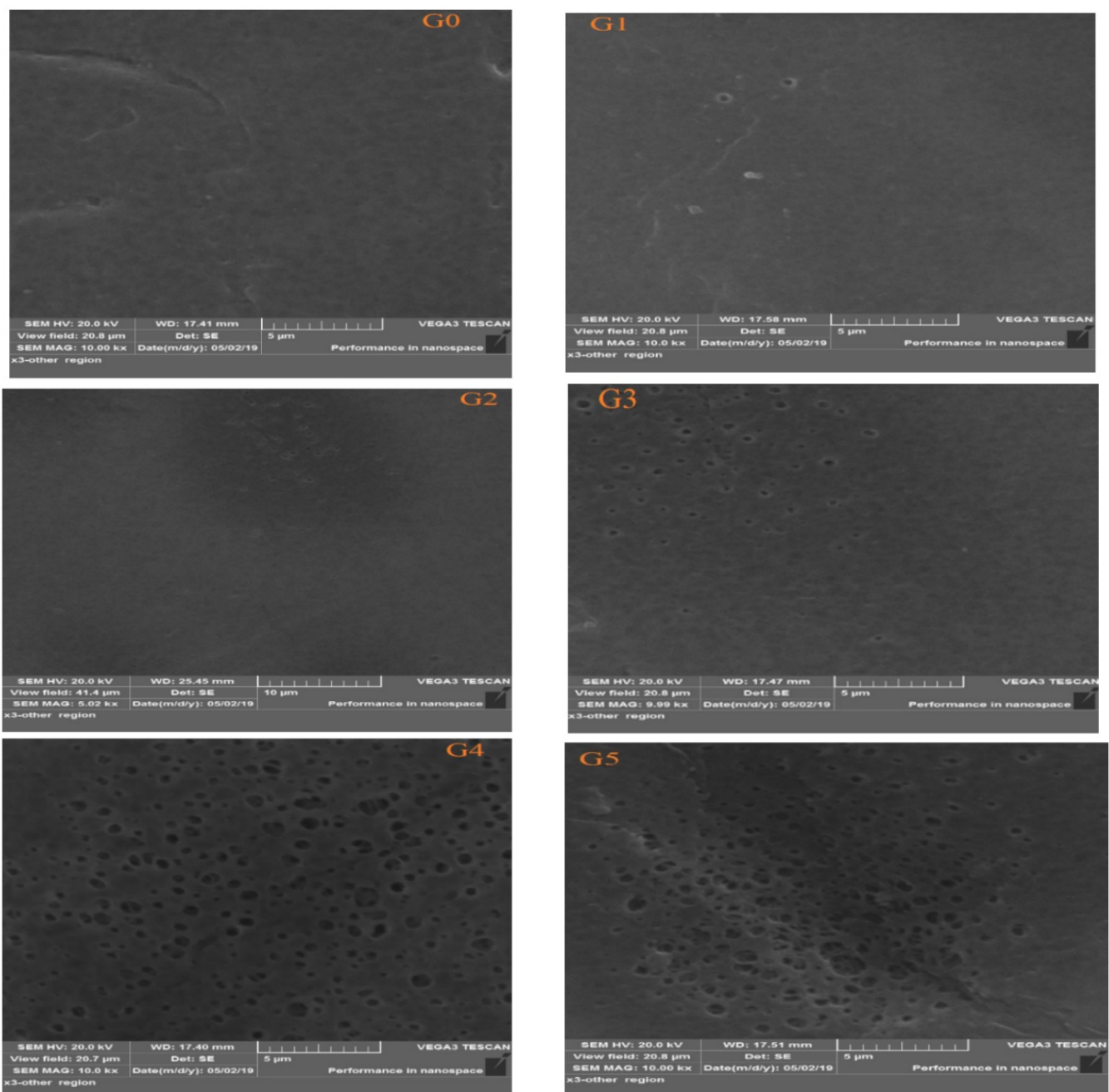


Figure 7. Cont.

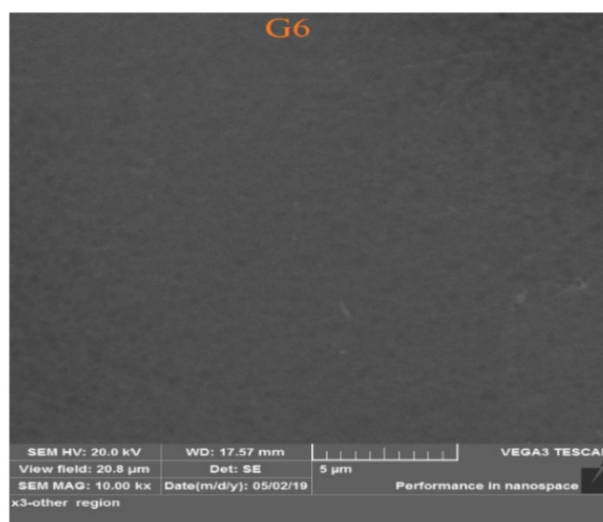


Figure 7. Top surface structures SEM images of the neat and PES/TGF membranes with various TGF nano-polymer contents ((G0) 20/0, (G1) 20/1, (G2) 20/2, (G3) 20/3, (G4) 20/4, (G5) 20/5, (G6) 20/6).

It is worth noting that the presence of TGF nano-polymer in the membrane dope solution did not have a substantial effect on the thick layer of the manufactured membrane.

4.4. Membrane Porosity and Wettability

Membrane features of surface wettability and hydrophilicity were examined via the measurement of contact angle between the distilled water droplets and the membrane surface, where a low contact angle refers to high hydrophilicity of the membrane. This effective variable plays a vital role in the entire membrane performance [26]. The contact angles of the pure PES and PES/TGF membranes were estimated, and the results are given in Figure 8 (right). The pristine membrane contact angle was 69.44° , showing the typical value of a pristine PES membrane. This magnitude showed a clear decrease to 51.7° upon adding 1 wt.% of TGF nano-polymer. As the content of the TGF in the polymeric solution increased, the contact angle decreased, clearly indicating an additional increase in the membrane surface hydrophilicity. Moreover, upon embedding 4 wt.% TGF nano-polymer, the water contact angle value was recorded at about 48° , showing a considerable enhancement in the hydrophilicity and wettability characteristics of the membrane. This amelioration is related to the increment in pore size and pore size distribution, as well as pore density. This led to an increase in the nanocomposite membrane hydrophilicity as a result of improved porosity. A further increase in the amount of TGF to 5 and 6 wt.% revealed a continuous slight increase in the values of contact angle to about 51° and 52° , respectively. This was induced by the decreased porosity obtained at higher casting solution viscosity, as the contact angle value relies on the interplay of several characteristics, such as surface porosity and pore size.

Figure 8 (left) illustrates the effect of TGF nano-polymer content in the polymer dope solution on the porosity of the prepared membrane. Upon adding 1 wt.% TGF nano-polymer into the PES polymer casting solution, the porosity of the membrane improved from 63.8% to 70.4%. Increasing the TGF concentration up to 4 wt.% resulted in improving the membrane porosity up to 73%. The improvement of membrane porosity following the addition of hydrophilic additives was also elucidated by Manawi et al. [27], who revealed that adding hydrophilic particles in the polymer dope solution produced an accelerated solvent/nonsolvent exchange rate, which in turn led to the enhancement of a highly porous membrane structure. Adding TGF nano-polymer led to growing thermodynamic instability in coagulation bath, thus eliminating the dense top layer and enhancing the porosity of the membrane surface. This also progressively changed the voids shape from the macrocavities in the PES membranes to the finger-like voids with a narrower size distribution in the

PES/TGF nano-polymer membranes. Until now, the formation of voids in polymer matrix has been attained in different ways, including the selective decomposition of thermally labile blocks from block copolymers, the selective decomposition of thermally unstable components from polymer blends, or the addition of porogens during the polymerization process. A higher porosity of the blend polymer membrane results in a lower impedance to the water flow across the membrane [28]. Higher membrane porosity may be relevant to a higher pore density. The further augment in TGF loading (>4 wt.%) reduced the porosity of the synthesized membrane. This can be interpreted by the increase in the viscosity of the polymer dope solutions, slowing down the precipitation process.

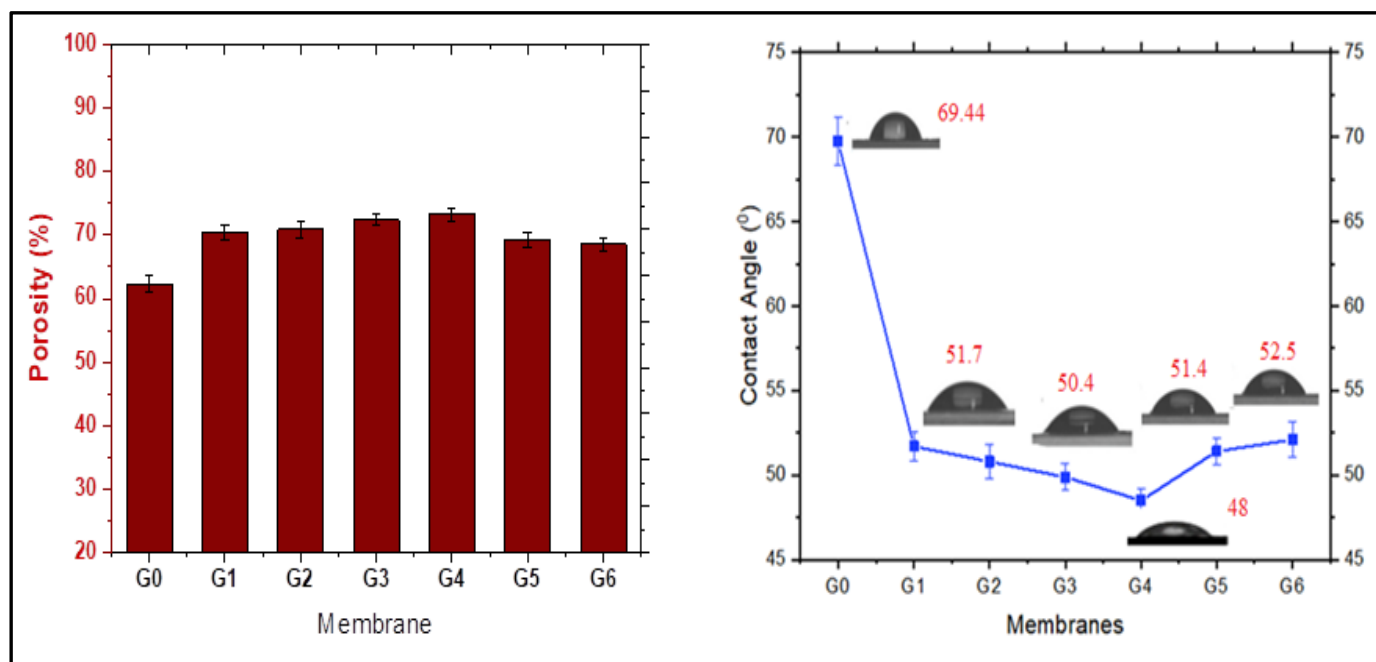


Figure 8. (Left) the effects of TGF content on the porosity of PES/TGF blend membranes; (Right) contact angle of PES membranes with various TGF concentrations.

4.5. Membrane Pore Size

The membrane pore size is illustrated in Figure 9. The pore size values of membranes G0, G1, G2, G3, G4, G5, and G6 were 20.35, 24.52, 32.94, 38.48, 39.56, 40.59, and 33.95 nm, respectively. Membrane pore size relies on the separation rate of the solution phase. In short, the addition of the pore former reduced the solvents exchange rate during the separation phase, resulting in the formation of large pores. Hence, the TGF nano-polymer was the primary contributing factor for the formation of highly porous membranes.

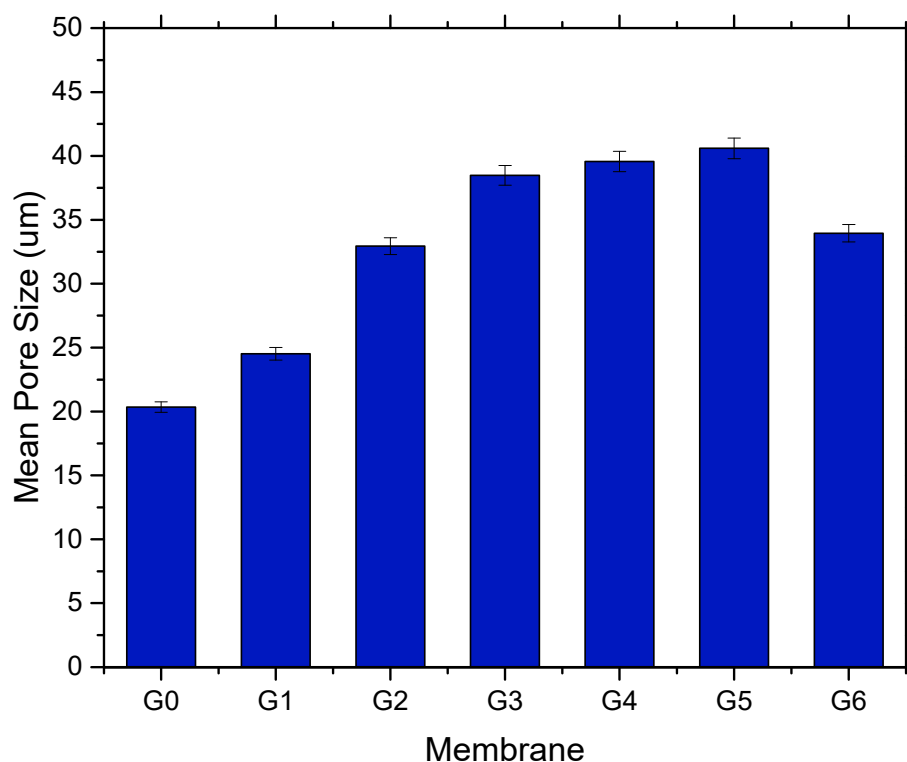


Figure 9. The pore size of the PES/TGF membranes with different contents of TGF nano-polymer.

4.6. Membrane Performance

4.6.1. Pure Water Flux

Pure water flux (PWF) and solute retention have a close relationship with the effect of pore size on the membrane surface (top layer porosity) and the pore density [29]. Generally, the outcomes exhibited that the PWF of the modified membrane could be considerably improved upon increasing the content of TGF nano-polymer in the casting solution (Figure 10 (left)). Changes in membrane structure cause variations in the separation performance. Figure 10 (left) illustrates the pure water fluxes of PES/TGF membranes with the various nano-polymer TGF contents. Pure water fluxes of PES/TGF membranes increased progressively with increasing TGF content (0–4 wt.%) in the dope casting solution, which may have resulted from the increase in the surface hydrophilicity, surface pore density, porosity, and macrovoids, as well as the formation of preferable vertically interconnected finger-like pores compared to those in the PES membrane [30]. The PWF of the mixed membranes was improved as a result of the increase in membrane hydrophilicity, which in turn enhanced the attraction and the affinity of water molecules in relation to the membrane morphology [31]. Results demonstrated that the PWF of the PES/TGF composite membrane exhibited a considerable amelioration (200%) compared with the PES pristine membrane. The water-soluble nano-polymer particulates accelerated the nonsolvent (water)/solvent exchange rate during the preparation stage, resulting in the formation of membranes with higher porosity and larger cavities. Accordingly, the membrane PWF and the permeation performance values were boosted. Furthermore, the alterations in the membrane cross-morphology in the presence of the nano-polymer particles, from the tiny finger-shaped pores (for the neat PES membrane) to the larger finger-shaped pores conjugated with macrovoids (for PES/TGF membranes), provided a smoother penetration situation for water molecules, enhancing the PWF. As clearly observed, the PWF of the PES/TGF membranes was improved after increasing the content of TGF in the casting solution up to 4 wt.%, and the highest value was associated with the ratio of 20/4 wt.% PES/TGF membrane. Unfortunately, when replacing the feed solution with BSA solution in lieu of distilled water, this resulted in a drastic decrease in the membrane permeate flux.

This can be attributed to the narrowing and blockage of the pores caused by BSA adsorption on the membrane surface [32]. The main cause was the presence of TGF particles in higher quantities, resulting in a rougher surface of the modified membrane, which was easily contaminated by BSA [33]. Subsequently, the membrane permeate flux decreased with higher loadings of TGF, which may have been due to the decreased contact angle and the increased porosity of the membrane. As is obvious in Figure 10 (left), the alteration of BSA solution flux for all membranes had a similar trend to that of the PWF. The membrane modified with 4 wt.% TGF illustrated the optimal value of BSA solution flux.

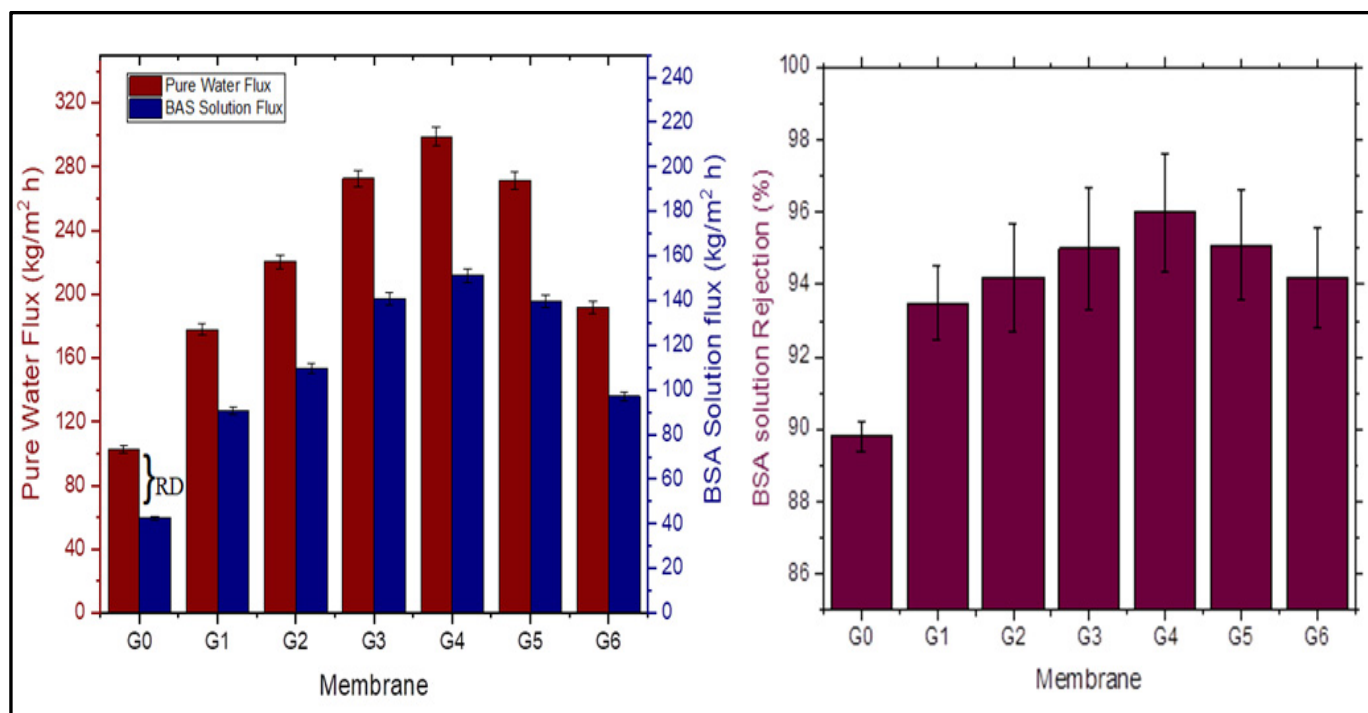


Figure 10. (Left) the water and BSA solution flux of the neat PES and PES/TGF membranes; flux reduction for G0 = 42%, G1 = 30%, G2 = 31%, G3 = 25%, G4 = 31%, G5 = 29%, and G6 = 29%. (Right) BSA solution retention for the neat PES and PES/TGF membranes.

4.6.2. BSA Rejection

Retention of the modified membranes against BSA protein solution is shown in Figure 10 (right). A BSA solution of 1000 ppm was chosen to evaluate the retention capacity for all experiments. All the TGF-modified membranes manifested a rejection value of higher than 91%. Impregnation of TGF at 4 wt.% disclosed the greatest BSA retention (above 96%) compared to 89.9% for the neat PES membrane, as can be seen in Figure 10 (right). This observed increase in the BSA removal for the PES/TGF membranes can be attributed to the effects of the addition of TGF to the membrane matrix, which imparted a greater hydrophilic nature to the surface of the membrane. This could have led to lower affinity and interactions between the membrane surface and BSA solution, thus improving membrane rejection. A slight change in this trend was witnessed after the addition of 5 and 6 wt.% TGF into the dope solution, which led to a slight reduction in the rejection values. This could be attributed to the reduction in the hydrophilicity of the membrane.

4.6.3. Long-Term Membrane Stability

One of the most questionable concerns about the performance of any membrane is its long-term stability under harsh operations. Membrane stability and its long-term operation were tested using 1000 ppm BSA solution. As can be seen in Figure 11, the permeate flux significantly decreased following the testing of the membranes using the BSA feed

solution. The permeation fluxes of the membranes decreased gradually as the filtration time passed, followed by a long period with a steady value. The reduction in flux rate did not exceed 16.8% for the improved membranes; 14% was the lowest value for the G4 membrane compared to 29.5% for the unmodified membrane (G0). This leads to the conclusion that the modification of the membranes via TGF nano-polymer had a more favorable antifouling performance. The long-term stability outcomes suggest that membrane matrices may have undergone textural structural alterations and/or accumulation of BSA particle residues, which resulted in pore clogging. However, this long-term experiment successfully proved that the membranes are still eligible for separating BSA solution under these processing conditions.

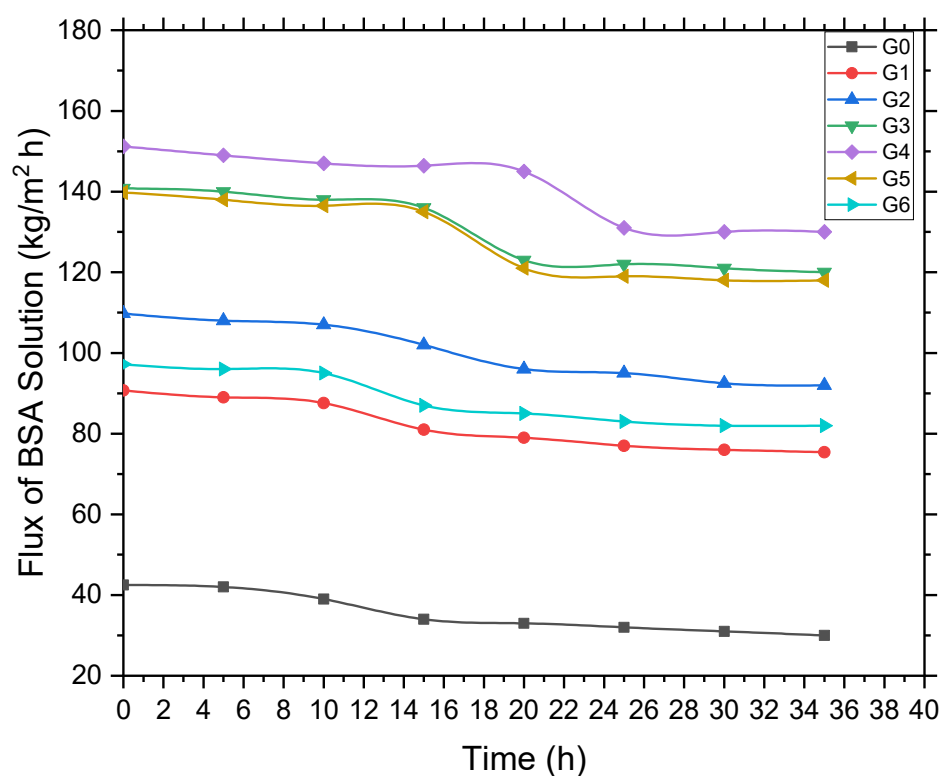


Figure 11. Permeate fluxes of the membrane as a function of exposure time over 250 h of 1000 ppm BSA feed solution.

4.7. Comparison Study

Table 2 shows the performance comparison of PES/TGF membranes prepared in the current work, using a novel TGF as a pore former, with those prepared using different pore formers presented in the literature. The values of the most considerable characteristics of the membranes, e.g., mean pore size, contact angle, and porosity, are presented in Table 2. It can be observed clearly that the novel PES/TGF membranes had a higher pure water flux and rejection efficiency compared to the most commonly used membranes found in the literature.

Table 2. Comparison of the membrane performance in this study with that of diverse membranes prepared in the literatures, regarding the pure water flux, retention percentage, and membrane characteristics.

Membrane	Pore Former	Membrane Characteristics			Membrane Performance		Process	Reference
		Mean Pore Size (nm)	Porosity (%)	Contact Angle (°)	PWP (kg/m ² ·h)	Rejection (%)		
PES	TGF	40.59	73.3	50.4	300	BSA 96	UF	This study [34]
PES	Silica-PVP	—	—	52.6	165	BSA 100	UF	
PVDF-HFP	Lithium chloride (LiCl)	7.85	—	79	51	Dextran aqueous solution 90	UF	[35]
PES	Pluronic F127	—	—	58	125	BSA 98	UF	[36]
PES	PVP	—	—	51.9	45	BSA 88	UF	[37]
PVDF	Water	580	79	141	11.6	NaCl 99.9	UF (MD)	[38]
PES	Sodium dodecyl sulfate (SDS)	6.8	—	54	230	—	UF	[39]
PES	Reverse triblock Pluronic GO/5P31R1	—	87	54	125	BSA 97	UF	[40]
PES	PEG	73.2	35.31	—	36.9	BSA 93.3	UF	[41]
PVDF	PEG	—	—	—	78.94	Dye 90.3	NF	[42]
PES	CC-Fe ₃ O ₄ NPs/PVP	5.5	86.3	52.5	36	Dye 99	NF	[43]
PSF	SiO ₂	10.7	78	71.3	55	2000 ppm NaCl solutions 99.1	RO	[44]
PVDF	MOF-199/PEG	50	80.89	85	185.05	BSA 94	UF	[45]
PES/PAN	PVP/PEG	—	55	76	100	Humic acid 92	UF	[46]
PES	Acacia gum (AG)	8.3	79	63	70	Lead 85	UF	[27]

5. Conclusions

In this work, polyethersulfone (PES) ultrafiltration membranes were improved using a novel water-soluble nano-polymer for protein separation applications. TGF was employed as a pore former, aiming to restructure the performance of the membrane. The classical phase separation technique was utilized to prepare various membrane compositions. The influence of various TGF contents (0–6 wt.%) on the structure, surface features, and performance of the neat and PES/TGF composite membranes was evaluated. Noticeably, the finger-form cavities through the structure of the neat PES membrane were changed into macrovoids, while the size and the number of the finger-like pores increased upon increasing the dosage of TGF. Additionally, the obtained outcomes revealed that increasing the TGF content in the casting solution promoted the permeability of the synthesized membranes, due to the improvement of porosity, hydrophilicity, and pore density. The modified membrane permeability was considerably enhanced, whilst still having good rejection. When the loading ratio of the TGF nano-polymer was 4%, the PWF of the modified membrane reached up to 298 kg·m^{−2}·h^{−1}, while rejection was close to 97% for the BSA solution. According to the obtained results, utilizing TGF as a water-soluble copolymer for the modification of PES membrane could produce a novel membrane that can withstand harsh operating conditions and long-term industrial operation in wastewater treatment applications.

The fouling phenomenon of the membrane represents the most significant dilemma to be taken into account affecting the performance of the UF membrane for different applications. The preparation of a novel and green water-soluble polymer acting as a pore former can be considered as a valuable way of modifying the structural morphology of membranes to overcome this phenomenon.

Author Contributions: Conceptualization, Q.F.A. and K.T.R.; methodology, Q.F.A., H.S.M., J.M.A. and K.T.R.; software, H.M.A. and A.E.M. validation, Q.F.A., K.T.R., J.M.A. and M.N.A.-B.; formal analysis, M.N.A.-B. and A.E.M.; investigation, Q.F.A., I.K.S., K.T.R. and M.N.A.-B.; writing—original draft preparation, Q.F.A., I.K.S., K.T.R. and M.N.A.-B.; writing—review and editing, Q.F.A., H.S.M. and I.K.S.; supervision, Q.F.A. and K.T.R. All authors have read and agreed to the published version of the manuscript.

Funding: This research received no external funding.

Data Availability Statement: Not applicable.

Conflicts of Interest: The authors declare no conflict of interest.

References

- Al-Ani, F.H.; Alsathy, Q.F.; Raheem, R.S.; Rashid, K.T.; Figoli, A. Experimental Investigation of the Effect of Implanting TiO₂-NPs on PVC for Long-Term UF Membrane Performance to Treat Refinery Wastewater. *Membranes* **2020**, *10*, 77. [\[CrossRef\]](#) [\[PubMed\]](#)
- Yu, H.; Li, X.; Chang, H.; Zhou, Z.; Zhang, T.; Yang, Y.; Liang, H. Performance of hollow fiber ultrafiltration membrane in a full-scale drinking water treatment plant in China: A systematic evaluation during 7-year operation. *J. Membr. Sci.* **2020**, *613*, 118469. [\[CrossRef\]](#)
- Fan, Z.; Wang, Z.; Sun, N.; Wang, J.; Wang, S. Performance improvement of polysulfone ultrafiltration membrane by blending with polyaniline nanofibers. *J. Membr. Sci.* **2008**, *320*, 363–371. [\[CrossRef\]](#)
- Olewi, A.H.; Jabur, A.R.; Alsathy, Q.F. Preparation of Polystyrene/Polyacrylonitrile Blends by Electrospinning Technique. *J. Phys. Conf. Ser.* **2021**, *1879*, 022065. [\[CrossRef\]](#)
- Aljumaily, M.M.; Alsaadi, M.A.; Hashim, N.A.; Alsathy, Q.F.; Mjalli, F.S.; Atieh, M.A. PVDF-co-HFP/superhydrophobic acetylene-based nanocarbon hybrid membrane for seawater desalination via DCMD. *Chem. Eng. Res. Des.* **2018**, *138*, 248–259. [\[CrossRef\]](#)
- Aljumaily, M.M.; Alsaadi, M.A.; Hashim, N.A.; Alsathy, Q.F.; Das, R.; Mjalli, F. Embedded high-hydrophobic CNMs prepared by CVD technique with PVDF-co-HFP membrane for application in water desalination by DCMD. *Desalination Water Treat.* **2019**, *142*, 37–48. [\[CrossRef\]](#)
- Jamed, M.J.; Alanezi, A.A.; Alsathy, Q.F. Effects of embedding functionalized multi-walled carbon nanotubes and alumina on the direct contact poly(vinylidene fluoride-cohexafluoropropylene) membrane distillation performance. *Chem. Eng. Commun.* **2019**, *206*, 1035–1057. [\[CrossRef\]](#)
- Al-Araji, D.D.; Al-Ani, F.H.; Alsathy, Q.F. Modification of polyethersulfone membranes by Polyethyleneimine (PEI) grafted Silica nanoparticles and their application for textile wastewater treatment. *Environ. Technol.* **2022**. [\[CrossRef\]](#)
- Xu, Z.L.; Qusay, F.A. Effect of polyethylene glycol molecular weights and concentrations on polyethersulfone hollow fiber ultrafiltration membranes. *J. Appl. Polym. Sci.* **2004**, *91*, 3398–3407. [\[CrossRef\]](#)
- Rekik, S.B.; Gassara, S.; Bouaziz, J.; Deratani, A.; Baklouti, S. Enhancing hydrophilicity and permeation flux of chitosan/kaolin composite membranes by using polyethylene glycol as porogen. *Appl. Clay Sci.* **2019**, *168*, 312–323. [\[CrossRef\]](#)
- Yoo, S.H.; Kim, J.H.; Jho, J.Y.; Won, J.; Kang, Y.S. Influence of the addition of PVP on the morphology of asymmetric polyimide phase inversion membranes: Effect of PVP molecular weight. *J. Membr. Sci.* **2004**, *236*, 203–207. [\[CrossRef\]](#)
- Zhao, W.; He, C.; Wang, H.; Su, B.; Sun, S.; Zhao, C. Improved antifouling property of polyethersulfone hollow fiber membranes using additive of poly(ethylene glycol) methyl ether-b-poly (styrene) copolymers. *Ind. Eng. Chem. Res.* **2011**, *50*, 3295–3303. [\[CrossRef\]](#)
- Shi, Q.; Meng, J.-Q.; Xu, R.-S.; Du, X.-L.; Zhang, Y.-F. Synthesis of hydrophilic polysulfone membranes having antifouling and boron adsorption properties via blending with an amphiphilic graft glycopolymer. *J. Membr. Sci.* **2013**, *444*, 50–59. [\[CrossRef\]](#)
- Babatunde, A.A.; Obaid, M.; Yu, H.-W.; Kim, I.S. High-flux ultrafiltration membrane with open porous hydrophilic structure using dual pore formers. *Chemosphere* **2019**, *227*, 662–669. [\[CrossRef\]](#)
- Hussein, S.S.; Ibrahim, S.S.; Toma, M.A.; Alsathy, Q.F.; Drioli, E. Novel chemical modification of polyvinyl chloride membrane by free radical graft copolymerization for direct contact membrane distillation (DCMD) application. *J. Membr. Sci.* **2020**, *611*, 118266. [\[CrossRef\]](#)
- Ho, C.-C.; Su, J.F. Boosting permeation and separation characteristics of polyethersulfone ultrafiltration membranes by structure modification via dual-PVP pore formers. *Polymer* **2022**, *241*, 124560. [\[CrossRef\]](#)
- Alsathy, Q.F.; Rashid, K.T.; Ibrahim, S.S.; Ghanim, A.H.; Van der Bruggen, B.; Luis, P.; Zablouk, M. Poly(vinylidene fluoride-co-hexafluoropropylene) (PVDF-co-HFP) hollow fiber membranes prepared from PVDF-co-HFP/PEG-600Mw/DMAC solution for membrane distillation. *J. Appl. Polym. Sci.* **2013**, *129*, 3304–3313. [\[CrossRef\]](#)
- Alsathy, Q.F.; Merza, A.S.; Rashid, K.T.; Adam, A.; Figoli, A.; Simone, S.; Drioli, E. Preparation and Characterization of poly(vinyl chloride)/poly (styrene)/poly (ethylene glycol) hollow-fiber membranes. *J. Appl. Polym. Sci.* **2013**, *130*, 989–1004. [\[CrossRef\]](#)
- Ali, A.M.; Rashid, K.T.; Yahya, A.A.; Majdi, H.S.; Salih, I.K.; Yusoh, K.; Figoli, A. Fabrication of Gum Arabic-Graphene (GGA) Modified Polyphenylsulfone (PPSU) Mixed Matrix Membranes: A Systematic Evaluation Study for Ultrafiltration (UF) Applications. *Membranes* **2021**, *11*, 542. [\[CrossRef\]](#)

20. Farjami, M.; Vatanpour, V.; Moghadassi, A. Effect of nanoboehmite/poly (ethylene glycol) on the performance and physiochemical attributes EPVC nano-composite membranes in protein separation. *Chem. Eng. Res. Des.* **2020**, *156*, 371–383. [\[CrossRef\]](#)
21. Susanto, H.; Ulbricht, M. Characteristics, performance and stability of polyethersulfone ultrafiltration membranes prepared by phase separation method using different macromolecular additives. *J. Membr. Sci.* **2009**, *327*, 125–135. [\[CrossRef\]](#)
22. Wang, Z.; Wang, H.; Liu, J.; Zhang, Y. Preparation and antifouling property of polyethersulfone ultrafiltration hybrid membrane containing halloysite nanotubes grafted with MPC via RATRP method. *Desalination* **2014**, *344*, 313–320. [\[CrossRef\]](#)
23. Farahani, M.H.D.A.; Rabiee, H.; Vatanpour, V.; Borghei, S.M. Fouling reduction of emulsion polyvinylchloride ultrafiltration membranes blended by PEG: The effect of additive concentration and coagulation bath temperature. *Desalination Water Treat.* **2016**, *57*, 11931–11944. [\[CrossRef\]](#)
24. Wienk, I.M.; Boom, R.M.; Beerlage, M.A.M.; Bulte, A.M.W.; Smolders, C.A.; Strathmann, H. Recent advances in the formation of phase inversion membranes made from amorphous or semi-crystalline polymers. *J. Membr. Sci.* **1996**, *113*, 361–371. [\[CrossRef\]](#)
25. Boom, R.M.; Wienk, I.M.; Van den Boomgaard, T.; Smolders, C.A. Microstructures in phase inversion membranes. Part 2. The role of a polymeric additive. *J. Membr. Sci.* **1992**, *73*, 277–292. [\[CrossRef\]](#)
26. Haghighat, N.; Vatanpour, V.; Sheydaei, M.; Nikjavan, Z. Preparation of a novel polyvinyl chloride (PVC) ultrafiltration membrane modified with Ag/TiO₂ nanoparticle with enhanced hydrophilicity and antibacterial activities. *Sep. Purif. Technol.* **2020**, *237*, 116374. [\[CrossRef\]](#)
27. Manawi, Y.; Kochkodan, V.; Mahmoudi, E.; Johnson, D.J.; Mohammad, A.W.; Atieh, M.A. Characterization and Separation Performance of a Novel Polyethersulfone Membrane Blended with Acacia Gum. *Sci. Rep.* **2017**, *7*, 15831. [\[CrossRef\]](#)
28. Costacurta, S.; Biasetto, L.; Pippel, E.; Woltersdorf, J.; Colombo, P. Hierarchical porosity components by infiltration of a ceramic foam. *J. Am. Ceram. Soc.* **2007**, *90*, 2172–2177. [\[CrossRef\]](#)
29. Ma, Y.; Shi, F.; Ma, J.; Wu, M.; Zhang, J.; Gao, C. Effect of PEG additive on the morphology and performance of polysulfone ultrafiltration membranes. *Desalination* **2011**, *272*, 51–58. [\[CrossRef\]](#)
30. Safarpour, M.; Khataee, A.; Vatanpour, V. Preparation of a novel polyvinylidene fluoride (PVDF) ultrafiltration membrane modified with reduced graphene oxide/titanium dioxide (TiO₂) nanocomposite with enhanced hydrophilicity and antifouling properties. *Ind. Eng. Chem. Res.* **2014**, *53*, 13370–13382. [\[CrossRef\]](#)
31. Leo, C.P.; Lee, W.C.; Ahmad, A.L.; Mohammad, A.W. Polysulfone membranes blended with ZnO nanoparticles for reducing fouling by oleic acid. *Sep. Purif. Technol.* **2012**, *89*, 51–56. [\[CrossRef\]](#)
32. Rabiee, H.; Vatanpour, V.; Farahani, M.H.D.A.; Zarrabi, H. Improvement in flux and antifouling properties of PVC ultrafiltration membranes by incorporation of zinc oxide (ZnO) nanoparticles. *Sep. Purif. Technol.* **2015**, *156*, 299–310. [\[CrossRef\]](#)
33. Dmitrenko, M.; Atta, R.; Zolotarev, A.; Kuzminova, A.; Ermakov, S.; Penkova, A. Development of Novel Membranes Based on Polyvinyl Alcohol Modified by Pluronic F127 for Pervaporation Dehydration of Isopropanol. *Sustainability* **2022**, *14*, 3561. [\[CrossRef\]](#)
34. Sun, M.; Su, Y.; Mu, C.; Jiang, Z. Improved antifouling property of PES ultrafiltration membranes using additive of silica–PVP nanocomposite. *Ind. Eng. Chem. Res.* **2010**, *49*, 790–796. [\[CrossRef\]](#)
35. Shi, L.; Wang, R.; Cao, Y.; Liang, D.T.; Tay, J.H. Effect of additives on the fabrication of poly (vinylidene fluoride-co-hexafluoropropylene)(PVDF-HFP) asymmetric microporous hollow fiber membranes. *J. Membr. Sci.* **2008**, *315*, 195–204. [\[CrossRef\]](#)
36. Wang, Y.Q.; Wang, T.; Su, Y.L.; Peng, F.B.; Wu, H.; Jiang, Z.Y. Remarkable reduction of irreversible fouling and improvement of the permeation properties of poly (ether sulfone) ultrafiltration membranes by blending with pluronic F127. *Langmuir* **2005**, *21*, 11856–11862. [\[CrossRef\]](#)
37. Rahimpour, A.; Jahanshahi, M.; Khalili, S.; Mollahosseini, A.; Zirepour, A.; Rajaeian, B. Novel functionalized carbon nanotubes for improving the surface properties and performance of polyethersulfone (PES) membrane. *Desalination* **2012**, *286*, 99–107. [\[CrossRef\]](#)
38. Nthunya, L.N.; Gutierrez, L.; Nxumalo, E.N.; Mhlana, S.D. Water as the Pore Former in the Synthesis of Hydrophobic PVDF Flat Sheet Membranes for Use in Membrane Distillation. *Hydro Sci. Mar. Eng.* **2019**, *1*, 1346. [\[CrossRef\]](#)
39. Moziaa, S.; Czyżewska, A.; Sienkiewicz, P.; Darownaa, D.; Szymańska, K.; Zgrzebnicki, M. Influence of sodium dodecyl sulfate on the morphology and performance of titanate nanotubes/polyethersulfone mixed-matrix membranes. *Desalination Water Treat.* **2020**, *208*, 287–302. [\[CrossRef\]](#)
40. Abdel-Karim, A.; Leaper, S.; Alberto, M.; Vijayaraghavan, A.; Fan, X.; Holmes, S.M.; Gorgojo, P. High flux and fouling resistant flat sheet polyethersulfone membranes incorporated with graphene oxide for ultrafiltration applications. *Chem. Eng. J.* **2018**, *334*, 789–799. [\[CrossRef\]](#)
41. Amirilargani, M.; Saljoughi, E.; Mohammadi, T. Improvement of permeation performance of polyethersulfone (PES) ultrafiltration membranes via addition of Tween-20. *J. Appl. Polym. Sci.* **2010**, *115*, 504–513. [\[CrossRef\]](#)
42. Khajavian, M.; Salehi, E.; Vatanpour, V. Nanofiltration of dye solution using chitosan/poly (vinyl alcohol)/ZIF-8 thin film composite adsorptive membranes with PVDF membrane beneath as support. *Carbohydr. Polym.* **2020**, *247*, 116693. [\[CrossRef\]](#) [\[PubMed\]](#)
43. Zinadini, S.; Zinatizadeh, A.A.; Rahimi, M.; Vatanpour, V.; Zangeneh, H.; Beygzadeh, M. Novel high flux antifouling nanofiltration membranes for dye removal containing carboxymethyl chitosan coated Fe₃O₄ nanoparticles. *Desalination* **2014**, *349*, 145–154. [\[CrossRef\]](#)

-
44. Yan, W.; Wang, Z.; Wu, J.; Zhao, S.; Wang, J.; Wang, S. Enhancing the flux of brackish water TFC RO membrane by improving support surface porosity via a secondary pore-forming method. *J. Membr. Sci.* **2016**, *498*, 227–241. [[CrossRef](#)]
 45. Wang, H.T.; Ao, D.; Lu, M.C.; Chang, N. Alteration of the morphology of polyvinylidene fluoride membrane by incorporating MOF-199 nanomaterials for improving water permeation with antifouling and antibacterial property. *J. Chin. Chem. Soc.* **2020**, *67*, 1807–1817. [[CrossRef](#)]
 46. Abdallah, H.; Jamil, T.S.; Shaban, A.M.; Mansor, E.S.; Souaya, E.R. Influence of the polyacrylonitrile proportion on the fabricated UF blend membranes' performance for humic acid removal. *J. Polym. Eng.* **2018**, *38*, 129–136. [[CrossRef](#)]